DAVID TAYLOR MODEL BASIN
WASHINGTON, DC

DEPARTMENT OF THE NAVY

HYDROMECHANICS

O

AERODYNAMICS

O

STRUCTURAL MECHANICS

O

APPLIED MATHEMATICS

O

ACOUSTICS AND VIBRATION

MINIMUM PRESSURE ENVELOPES FOR MODIFIED NACA-66 SECTIONS WITH NACA a = 0.8 CAMBER AND BUSHIPS TYPE I AND TYPE II SECTIONS

by

Terry Brockett

Distribution of this document is unlimited.

HYDROMECHANICS LABORATORY

RESEARCH AND DEVELOPMENT REPORT

February 1966

Report 1780

MINIMUM PRESSURE ENVELOPES FOR MODIFIED NACA-66 SECTIONS WITH NACA a = 0.8 CAMBER AND BUSHIPS TYPE I AND TYPE II SECTIONS

by

Terry Brockett

Distribution of this document is unlimited.

February 1966

Report 1780

TABLE OF CONTENTS

LIST OF FIGURES

LIST OF TABLES

NOTATION

C	Chord length
$C_L = \dfrac{\text{lift}}{1/2 \rho U^2 C}$	Two-dimensional lift coefficient
$C_P = \dfrac{p - p_\infty}{1/2 \rho U^2}$	Pressure coefficient
$f = \dfrac{\text{max. camber}}{\text{chord}}$	Maximum camber ratio
P	Local static pressure on section
P_∞	Free-stream static pressure
P_v	Vapor pressure of the liquid
U	Velocity of section
x	Fraction of chord measured from leading edge
Y_T	Thickness ordinate, fraction of chord
Y_C	Camberline ordinate, fraction of chord
α	Angle of attack
ρ	Fluid mass density
$\rho_{LE} = \dfrac{\text{LE radius}}{\text{chord}}$	Nondimensional leading edge radius
$\sigma = \dfrac{P_\infty - P_v}{1/2 \rho U^2}$	Cavitation number
$\tau = \dfrac{\text{max. thickness}}{\text{chord}}$	Thickness ratio (twice the maximum thickness ordinate)
$\varphi = \text{arc cos } (2x-1)$	Angular variable

ABSTRACT

Minimum pressure envelopes, computed for steady two-dimensional flow, with an empirical correction for viscosity, are presented in graphic form for three foils: NACA 66 (TMB modified nose and tail) thickness with the NACA a = 0.8 camberline, the BuShips Type I section and the BuShips Type II section. In addition, design charts for selecting an "optimum" foil are included. A comparison of these foils, designed to have a favorable operating range of minimum pressures for a specified cavitation number and lift coefficient, shows the 66 (modified) form to provide a slightly wider margin for angle changes. Also with zero camber, the 66 (modified) section has a greater range of favorable minimum pressures than the other foils.

ADMINISTRATIVE INFORMATION

This work was funded by BuShips Subproject S-F013-1109, Task 3802, (TMB Problem No. 526-076).

INTRODUCTION

If it is assumed that cavitation will first occur on a body when the local pressure falls to the vapor pressure of the surrounding liquid, a knowledge of the minimum pressure is sufficient to predict the onset of cavitation or to design cavitation-free foils. Although the basic assumption that cavitation occurs at vapor pressure is not verified experimentally, at least for the low Reynolds numbers ($\sim 10^6$) encountered in laboratory tests, predictions are generally conservative and agreement between experimental results and theoretical predictions improves with increasing Reynolds number.[1*] Hence, there is some hope that the minimum pressure will be

* References are listed on page 12.

adequate for predicting surface cavitation at the higher Reynolds numbers encountered in full-scale applications.*

This report presents two-dimensional minimum pressure envelopes for three foils. The method of computing the pressure distribution is explained in Reference 1 and consists of calculating the potential flow pressure with an empirical correction for viscosity; the potential theory is modified to allow for arbitrary lift at a given angle of incidence, and the required lift is determined from estimates of the angle of zero lift and lift-curve slope.

DESCRIPTION OF FOILS

Three profiles commonly in use for propeller blade sections were chosen for the present study. These profiles are the NACA 66 (TMB modified) thickness distribution with the NACA a = 0.8 camberline, the BuShips Type I, and the BuShips Type II sections.

The basic NACA 66 (TMB modified) section is the NACA 66-006,[2] thickened[3] near the trailing edge for ease of manufacture (a parabola is fitted from the position of maximum thickness to a finite trailing edge offset). Ordinates of the thickness distribution vary linearly with maximum thickness ratio. When the pressure distribution on the NACA 66-006 was calculated using the computed program of Reference 1, a sharp suction peak was discovered near the leading edge (see Figure 1). If the ordinates are plotted at the angular stations φ = arc cos (2x-1) instead of the usual x, a slight hump appears at the leading edge (Figure 2) which causes the pressure peak. A similar, though smaller, pressure peak on the NACA

* Full-scale cavitation usually occurs at considerably higher cavitation numbers than predicted from either theory or model tests. The differences are attributed to manufacturing tolerances, inaccurate modeling of inflow velocities, and/or scale effect. Naturally the above conjecture applies to accurately constructed foils with smooth, fair surfaces operating in a steady uniform stream.

65A006 was noted in Reference 4 and also in Reference 1. (The hump is thought to be the result of inaccuracies in the numerical method used for the design of the NACA 6 Series foils.[1]) The nose hump on the 66 section was faired out by trial and error to give a smooth pressure curve. Ordinates for the final foil, modified nose and tail, are tabulated in Table 1 as well as values for the NACA a = 0.8 camberline.[2] The calculated nonviscous pressure distribution on this modified thickness distribution at zero incidence is shown in Figure 3 for a foil of 10-percent thickness. For this section, the ordinates of cambered foils are obtained by laying off the thickness perpendicular to the camberline at the corresponding station.

The BuShips Type I* section[5] is a modified NACA 16 section[2] with parabolic-arc camber (NACA 65 meanline[2]). The thickness distribution is the same as the "16" up to mid-chord; from the mid-chord to the trailing edge a parabola is fitted (the trailing edge is thinner than the "16"). The BuShips Type II* section[6] is the NACA 16 thickness form[2] and the parabolic-arc camber. Section ordinates are obtained by adding and subtracting the thickness ordinate from the camberline ordinate (i.e., thickness is added perpendicular to the nose-tail line). Thickness and camberline ordinates are tabulated in Table 2 for the BuShips foils. An equation for the NACA 16 thickness form which permits analytic determination of the ordinates can be found in Reference 1.** Calculated nonviscous pressure distributions on the basic thickness forms of 10-percent thickness are shown in Figure 4.

In Table 3 offsets for the three foils are tabulated at conventional stations.

---

* In practice, both the Type I and Type II sections have a modification near the trailing edge for strength purposes.[5,6] However, this modification depends upon the particular design and cannot be handled in general. The simplest case of no modification is considered in this report.

** Several other equations for the NACA 16 sections are available; for example, see NACA Technical Note 1546 and ARC C.P. No. 68.

The minimum pressure envelopes of this report supersede the previously computed values[7] for the two BuShips foils. The minimum pressures in that report were calculated using a computer program which did not determine pressures at enough points near the nose to ensure obtaining the minimum value. The computer program developed in Reference 1 corrects this deficiency.

CALCULATION OF MINIMUM PRESSURE ENVELOPES

The pressure distribution about each cambered foil was calculated[1] for various angles of attack between -5 and +6 degrees. For symmetrical foils, the pressure distribution was calculated for various angles from 0 to 8 degrees. At each angle of attack, the minimum of the computed pressures was selected. The enclosed figures are plots of $-C_{p_{min}}$, the negative of the minimum pressure coefficient versus α, the angle of incidence measured from a line joining the camberline endpoints.

The calculation of the pressure distribution depends upon specifying a lift coefficient C_L for a given angle of incidence. When the experimental lift is used, good agreement with measured pressure distributions is obtained.[1] The experimental lift can be determined from a lift-curve slope and angle of zero lift:

$$C_L = 2\pi \eta (\alpha - \alpha_{o_e}) \qquad [1]$$

where η is the lift-curve slope coefficient, $\frac{dC_L}{d\alpha}/2\pi$, and

α_{o_e} is the experimental angle of zero lift.

Analysis[2] of experimental data obtained at a relatively large Reynolds number (6×10^6) shows that η and α_{o_e} are independent of each other within the limits of experimental scatter, that η depends upon the thickness distribution, and that α_{o_e} is approximately a constant fraction of the nonviscous thin-wing value.

Since the lift-curve slope increases with increasing Reynolds number,[8] a value of η near unity is reasonable at the high Reynolds number ($\sim 10^8$) at which these foils are expected to operate. Also, it is reasonable to expect that the large trailing edge thickness of the modified 66 form would cause η to be lower for that foil than for the other two foils. Since the trailing edge of the BuShips Type II section (NACA 16) is similar to the NACA 4-digit series, the slope coefficient η was taken as $(1 - 0.61\tau)$, i.e., decreasing linearly with the thickness ratio τ, which is approximately the value for the NACA 4-digit series at a Reynolds number of 6×10^6. In the absence of specific test data, the BuShips Type I section was assumed to behave as the Type II section. For the modified 66 foil, η was estimated to be $(1 - 0.83\tau)$, which is slightly lower than the slope coefficient for the BuShips foils.

The actual angle of zero lift α_{o_e} for the NACA a = 0.8 camberline is 1.05[3*] times the thin-wing value[2] of zero lift, or

$$\alpha_{o_e} = 1.05\,(-1.95\,f) = -2.05\,f \quad \text{radians!}$$

and for the parabolic-arc camberline the angle of zero lift is about 0.93[2] times the thin-wing value or

$$\alpha_{o_e} = 0.93\,(-2\,f) = -1.86\,f$$

where α_{o_e} is in radians and f is the maximum camber ratio.

When these quantitites are substituted into the equation for lift, the expressions become

for the 66 foils: $$C_L = 2\pi\,(1 - 0.83\tau)\,(\alpha + 2.05\,f)$$

for the BuShips foils: $$C_L = 2\pi\,(1 - 0.61\tau)\,(\alpha + 1.86\,f) \qquad [2]$$

where α is in radians.

For convenience, the lift coefficient formulas are printed on the respective figures of minimum pressure envelopes for α in degrees.

---

* This investigator knows of only one test of the a = 0.8 camberline: that given on page 200 of Reference 9, in which the faired value of α_{o_e} is approximately 1.02 ± 0.07 times the thin-wing value. The above value of 1.05 is thus quite reasonable.

The minimum pressure envelopes obtained by specifying the above lift coefficients are plotted in Figures 5 through 11 for the modified 66 form and in Figures 12 through 18 for the BuShips forms. These curves are presented as $-C_{p_{min}}$ versus α ; for small changes in η and α_{o_e} , there is little change in minimum pressure. Also, in design work, the expected variation in angle of attack can often be predicted so that once a particular foil is selected, the extreme incidence can be used in the figures to check the suitability of the foil from a cavitation standpoint.

The significance of the shape of the $-C_{p_{min}} - \alpha$ curves is that in the region roughly parallel to the α axis, the minimum pressure occurs near mid-chord, and when the curve is roughly parallel to the $-C_{p_{min}}$ axis the minimum pressure is near the nose of the section. For the section with the a = 0.8 meanline, the displacement of the curves on the α scale is roughly related to the ideal angle of attack (the angle for which thin-wing theory predicts a stagnation point at the leading edge of the camberline).

Although the data are not given in this report, it was found that adding and subtracting the thickness from the camber, rather than applying the thickness perpendicular to the camber, resulted in higher $-C_{p_{min}}$ values and shifted the envelope slightly toward the higher α's. These effects are negligible for all but the highest thickness and camber ratios. Specifically there is a negligible difference in the envelopes for thickness ratios less than 0.1 or camber ratios less than 0.02.

DESIGN CHARTS

The figures may be used in two ways: first, and simpler, they may be used to predict cavitation on existing foils of the type considered, and second, they may be used to select foils which will not cavitate when operating over a specified range of angles.

In the first case, the camber, thickness, angle of attack, and operating cavitation number σ are known. From the foil geometry and the angle of attack, a minimum pressure coefficient is obtained from the minimum pressure envelopes given in this report. Cavitation is assumed not to occur when σ is greater than $-C_{P_{min}}$, and cavitation is assumed to occur when σ is less than $-C_{P_{min}}$.

To help in the foil selection from a cavitation standpoint, design charts (Figures 19, 20, and 21) were prepared graphically from the minimum pressure envelopes. The charts are based on the "optimum" foil, which is defined as the foil allowing the greatest total angle change without occurrence of cavitation for a given σ. For symmetrical foils (Figures 5 and 12), the "optimum" is clearly the profile for which the minimum pressure envelope changes from rising almost vertically from the $-C_{P_{min}}$ scale to going roughly parallel to it at the given $-C_{P_{min}}$, i.e., the "optimum" is the foil whose minimum pressure envelope touches the envelope* of the minimum pressure envelopes at the desired $-C_{P_{min}}$ or σ. For symmetrical foils, the permissible range of operating angles is twice the incidence ordinate of the envelope of the envelopes at the given $-C_{P_{min}}$ or σ (see Figures 5 and 12).

For cambered foils, there are two different envelopes to the minimum pressure envelopes, one for the upper surface and one for the lower surface. Since the one for the upper surface of the foil occurs at higher $-C_{P_{min}}$ values than does the one for the lower surface, it is used to determine the optimum foil. The width of the bucket is then that of the envelope at the given $-C_{P_{min}}$. Note that if σ (or $-C_{P_{min}}$) is expected to vary over the operating range of angles, then it would be better to use the original curves and not the design charts.

---

* The envelope of the minimum pressure envlopes can be expressed analytically as $\frac{\partial q}{\partial \tau} = 0$ where q is the velocity on the foil, and the expression is evaluated at the point of maximum velocity. Such an evaluation becomes too cumbersome for anything but very simple expressions for the velocity, and hence the envelope of envelopes was obtained graphically for the foils in this report.

The first of the charts (Figure 19) gives the "optimum" geometry of the 66 foils and the BuShips Type II section (since it is superior to the Type I). In addition, Figure 19 gives the width of the minimum pressure envelope in degrees for the "optimum" foil. For a specific type of section, given $-C_{P_{min}}$ or σ and given angle variation, there is a unique combination of camber ratio and thickness ratio for an "optimum" section.

The other design charts (Figures 20 and 21) give the operating incidence and lift coefficient for an "optimum" foil. Two different average operating conditons are considered: midpoint and 2:1 ratio. For midpoint operation, the foil will experience angle-of-attack variations of equal magnitude in the positive and negative directions about the operating incidence. For the 2:1 ratio, the foil will experience twice the positive variation as the negative (positive in the nose-up direction).*

In the design of cavitation-free foils, a design C_L is set, a minimum thickness from strength considerations is obtained, and a minimum operation σ is calculated.** In some cases a variation in the operating angle of attack is known or can be estimated. It is now necessary to find a camber ratio, thickness ratio, and an average operating angle of attack such that the design C_L is met, the thickness is not less than the strength considerations permit, and such that $-C_{P_{min}}$ is less than σ over the range of angle of attack variations. Actually, for the nonsteady problem, the nonsteady minimum pressures should be computed. This investigator knows of no "simple" method of doing this and hence the "quasi-steady" approach outlined above is suggested.

For situations when the angle-of-attack variation is not known or not critical, the following procedure is recommended: With the minimum thickness and known σ (i.e., $-C_{P_{min}}$), enter Figure 19 to obtain a camber ratio. Then enter Figure 20 or 21 with a selected type of angle variation to obtain an operating incidence and C_L. In general, this C_L will not be the same as

---

* A 2:1 angle variation is considered typical of propeller-blade sections.

** In certain cases, σ may vary, as in a nonuniform flow, and the minimum pressure envelopes - not the design charts - should be used.

that required. Either the thickness may be increased or the chord lengthened - or both - and the process repeated until the required C_L is obtained for an "optimum" foil.

If the angle-of-attack variation is known and critical, then the known variation and known σ uniquely determine τ and f from Figure 19. Figures 20 and 21 will give an operating incidence and C_L for the foil. Here too, it may be necessary to change the chordlength to carry the necessary load, remembering that the thickness and camber ratio are fixed. In propeller design, the fixed coefficient is the lift coefficient multiplied by the chord-diameter ratio. Once C_L is read, the chordlength is determined. If this section is close but does not quite make the strength requirements, a judicious rereading of the charts is suggested since some latitude is permitted in the readings. For large disagreements, designing for a smaller angle variation is suggested since experiments seem to indicate that the cavitation inception curve is wider than the minimum pressure envelope.[1]

The above procedures are not rigid, of course, and are offered only as a guide. It is quite possible that other design approaches will be used. In some instances perhaps the camber, σ, and incidence are fixed. In this case, Figure 19 will give an optimum thickness for the fixed σ and also the permissible angle variation. Figure 20 or 21 will give the midpoint of the envelope. The endpoint incidences of the envelope width would be the midpoint plus or minus one-half the width. These endpoints permit a check that the operating incidence is within their limits.

To illustrate and extend the remarks made in the previous paragraphs, a specific design problem will be presented. The problem is to determine a foil shape and incidence for a given C_L for the two types of foils considered in this section (i.e., 66 and Type II) and such that the minimum pressure envelopes extend approximately equal distances on both sides of the design angle of attack. For each foil, the average lift coefficient was taken to be 0.3 and σ (or $-C_{P_{min}}$) was taken to be 0.6.

For the 66 foil, Figures 19 and 20 are entered with σ and C_L, respectively, and a common thickness and camber ratio found. This gives a thickness ratio of 0.126, a camber ratio of 0.0225, and an operating incidence of 0.41 degrees. The second part of Figure 19 gives a total permissible angle variation of 3.9 degrees.

Similarly for the BuShips Type II foil, Figures 19 and 21 show an optimum foil with a thickness ratio of 0.119, a camber ratio of 0.0245, and an incidence of 0.34 degrees. From Figure 19, the total width of the envelope is seen to be 3.7 degrees.

The minimum pressure envelopes for these foils have been computed independently and are plotted in Figure 22. These curves are plots of $-C_{P_{min}}$ versus C_L to emphasize that each foil was selected to give the same C_L. These curves reinforce the above paragraphs in that they show the NACA 66 (modified) form to be superior to the BuShips Type II since its minimum pressure envelope permits a greater margin for angle changes before cavitation occurs. (The angle variation is the difference in lift coefficients divided by the lift-curve slope.)

In foil selection from a cavitation standpoint, several points are worth keeping in mind: First, for constant angle of attack in the favorable operating range (the nearly vertical line on the figures for which $-C_{P_{min}}$ is low), the value of $-C_{P_{min}}$ increases with both τ and f. Second, the extent, with respect to α, of the favorable range increases with increasing τ and also with increasing f. Third, in this favorable range, $-C_{P_{min}}$ increases more rapidly with f than with angle of attack for equal changes in C_L. Fourth, the thin-wing ideal angle of attack may be of limited use when designing cavitation-free foils to meet a given variation in angle of attack.* Fifth, often it will not be possible to avoid cavitation for a given σ and angle-of-attack variation.

---

* The use of the ideal angle of attack as the design incidence is based on the assumption that minimum drag occurs at this incidence. Unfortunately, experimental results[2] show this is only approximately true. Small departures from the "ideal" such as recommended here are still within the region of low drag.

SUMMARY AND CONCLUSIONS

Minimum pressure envelopes are presented in graphic form for three foils: the NACA 66 (TMB modified nose and tail) with the NACA a = 0.8 camberline, the BuShips Type I section and the BuShips Type II section. Without camber, the NACA 66 (modified) form has a greater extent of favorable operating range (i.e., lower $-C_{P_{min}}$ values) than do the BuShips foils. Cambered foils selected for the same operating conditions also show the 66 foil to be slightly superior to the BuShips foils. Over the entire range of thickness and camber ratios, the BuShips Type I has a higher $-C_{P_{min}}$ than does the Type II.

The theoretical calculations show that in the favorable operating range, increasing the thickness or camber ratio increases the value of $-C_{P_{min}}$ but the extent of the favorable operating range, with respect to α, is increased. In the favorable operating range, the calculations also show that $-C_{P_{min}}$ increases faster with camber ratio than with angle of attack for equal changes in lift coefficient.

Design charts, which give the "optimum" camber and thickness ratios for a given angle-of-attack variation or lift coefficient, and cavitation number are presented for the NACA 66 (modified) section and for the BuShips Type II section.

ACKNOWLEDGMENT

Mr. Jeffrey Morehouse provided invaluable assistance in the development of the design charts.

REFERENCES

1. Brockett, T., "Steady Two-Dimensional Pressure Distributions on Arbitrary Profiles," David Taylor Model Basin Report 1821 (Oct 1965).

2. Abbott, I. H. and von Doenhoff, A. E., "Theory of Wing Sections," Dover Publications (1959).

3. Eckhardt, M. K. and Morgan, W. B., "A Propeller Design Method," Transactions of the Society of Naval Architects and Marine Engineers (1955).

4. Hess, J. L. and Smith, A. M. O., "Calculation of the Non-Lifting Potential Flow about Arbitrary Three-Dimensional Bodies," Douglas Aircraft Co. Report No. ES-40622 (1962).

5. "Propeller Blade Section Design Coefficients for Type I Sections," BuShips Drawing Number 203-1737514 (21 Jul 1958).

6. "Propeller Blade Section Design Coefficients for Type II Sections," BuShips Drawing Number 203-1737515 (21 Jul 1958).

7. Caster, E. B., "Incipient Cavitation Diagrams for BuShips Type I and II Sections," David Taylor Model Basin Report 1643 (Jul 1962).

8. Riegels, F., "Airfoil Sections," Butterworths, London (1961).

9. Abbott, I. H., von Doenhoff, A. E., and Stivers, L. S., Jr., "Summary of Airfoil Data," NACA Report 824 (1945).

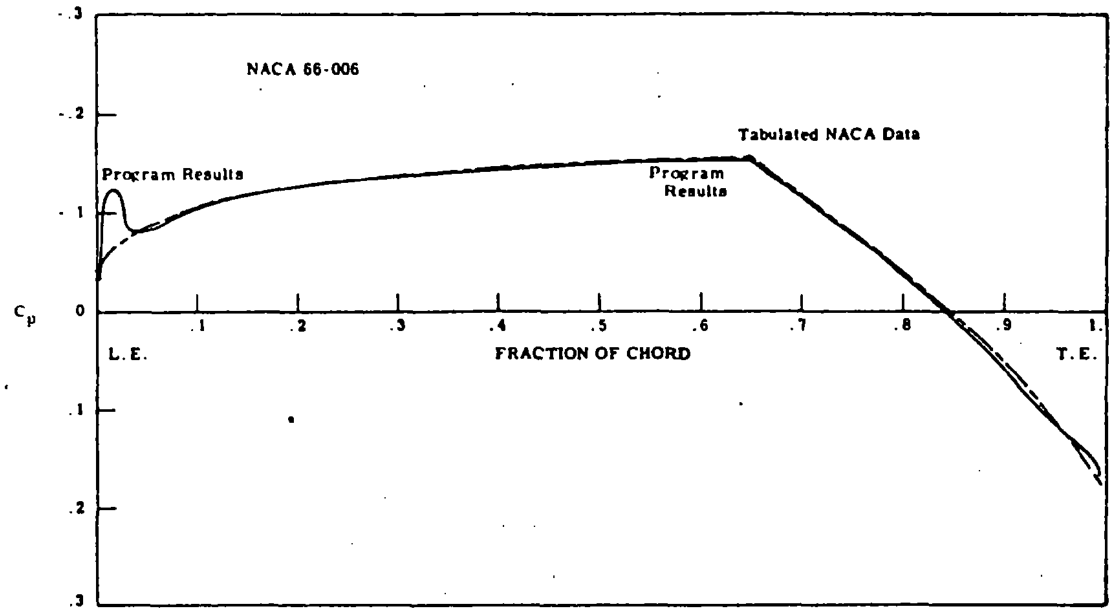

NACA 66 - 006

X	Y_p
.0	.0
.007596	.00557
.030154	.00999
.066987	.01442
.116978	.01884
.178606	.02287
.25	.02618
.328990	.02856
.413176	.02983
.5	.02985
.586824	.02847
.671010	.02501
.75	.01953
.821394	.01361
.883022	.00815
.933013	.00394
.969846	.00142
.992404	.00032
1.0	.0

Figure 1 - Pressure Distribution on the NACA 66-006 Showing Pressure Peak at Nose

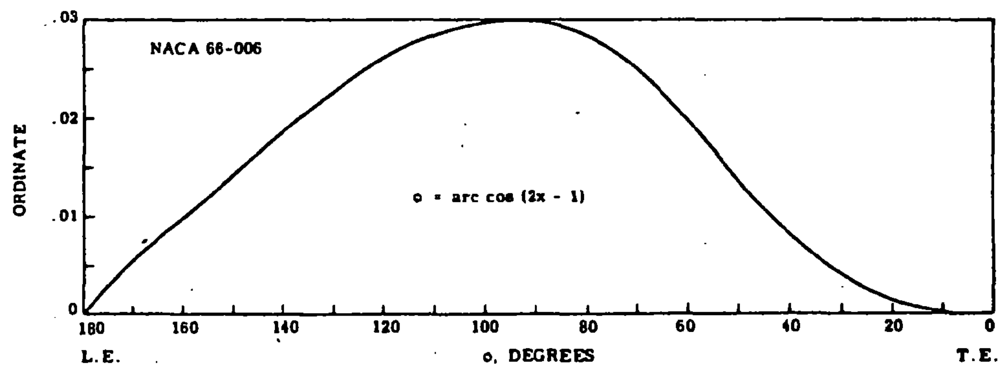

Figure 2 - Ordinate versus Angular Variable, Showing Hump near the Leading Edge, NACA 66-006

TABLE 1

Section Geometry, NACA 66 (Mod) and a = .8 Camber

Station x	66 (Mod) Thickness Y_T/t	a = .8 Camber Y_C/f	Camberline Slope $\frac{dY_C}{dx}/f$
0	0*	0	7.1485**
.007596	.0817	.06006	6.6001
.030154	.1608	.13381	4.7712
.066987	.2388	.33684	3.6751
.116978	.3135	.49874	2.8681
.178606	.3807	.65407	2.2096
.25	.4363	.79051	1.6350
.328990	.4760	.89831	1.1071
.413176	.4972	.96994	0.6001
.5	.4962	1.0	0.0914
.586824	.4712	.98503	-0.4448
.671010	.4247	.92306	-1.0483
.75	.3612	.81212	-1.6132
.821394	.2872	.63884	-3.1892
.883022	.2108	.42227	-3.7243
.933013	.1402	.23423	-3.7425
.969846	.0830	.09982	-3.5148
.992404	.0462	.02365	-3.2028
1.0	.0333	0	-3.0025

*ρ_{LE} = $\underbrace{.448}$ t^2 = C_N

**Value at x = .005

C_N = 0.5 for elliptic

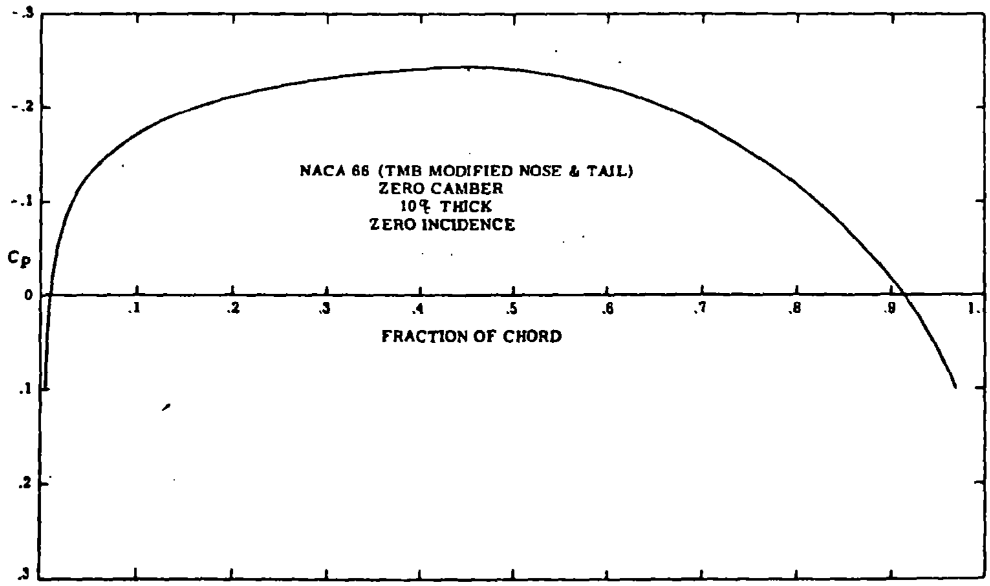

Figure 3 - Theoretical Pressure Distribution at α = 0 Degree on the NACA 66-010 (TMB Modified Nose and Tail)

TABLE 2

Section Geometry, BuShips Foils

Station x	Type I Thickness Y_T τ	Type II Thickness Y_T τ	Camber Ordinate Y_C f
0	0*	0*	0
.007596	.08438	.08438	.03015
.030154	.16451	.16451	.11698
.066987	.23969	.23969	.25
.116978	.30898	.30898	.41318
.178606	.37098	.37098	.58682
.25	.42370	.42370	.75
.328990	.46457	.46457	.88302
.413176	.49084	.49084	.96985
.5	.5	.5	1.0
.586824	.48493	.48977	.96985
.671010	.44151	.45674	.88302
.75	.375	.40031	.75
.821394	.29341	.32448	.58682
.883022	.20659	.23755	.41318
.933013	.125	.15084	.25
.969846	.05849	.07703	.11698
.992404	.01508	.02747	.03015
1.0	0	.01	0

$^*\rho_{LE} = .48889\,\tau^2$

C_N

C_N = 0.5 for [illegible]

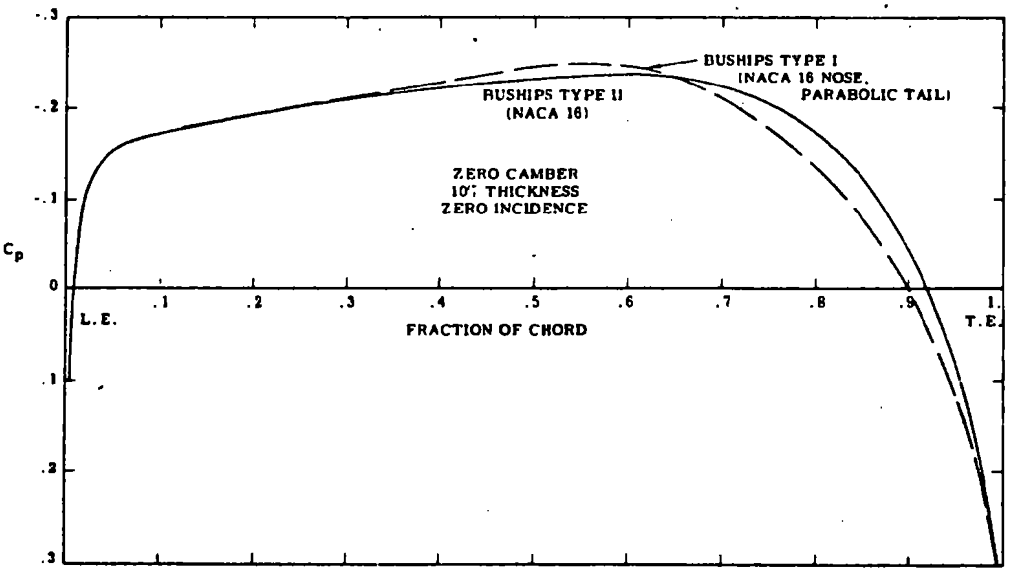

Figure 4 - Theoretical Pressure Distribution at [illegible] = 0 Degree on the BuShips Foils of 10-Percent Thickness and Zero Camber

TABLE 3

Foil Geometry at Conventional Stations

Station	NACA 66 (Mod) & a = .8 Camber			BuShips Foils		
	Thickness Ordinate	Camber Ordinate	Camber Slope	Type I Thickness	Type II Thickness	Camber Ordinate
x	Y_T/τ	Y_C/f	$\frac{dY_C}{dx}/f$	Y_T/τ	Y_T/τ	Y_C/f
0	0	0	—	0	0	0
.005	.0665	.0423	7.149	.06873	.06873	.0199
.0075	.0812	.0595	6.617	.08386	.08386	.029775
.0125	.1044	.0907	5.944	.10758	.10758	.049375
.025	.1466	.1586	5.023	.15039	.15039	.0975
.05	.2066	.2712	4.083	.20908	.20908	.19
.075	.2525	.3657	3.515	.25254	.25254	.2775
.1	.2907	.4482	3.100	.28800	.28800	.36
.15	.3521	.5869	2.488	.34455	.34455	.51
.2	.4000	.6993	2.023	.38859	.38859	.64
.25	.4363	.7905	1.635	.42370	.42370	.75
.3	.4637	.8635	1.292	.45145	.45145	.84
.35	.4832	.9202	0.933	.47275	.47275	.91
.4	.4952	.9615	0.678	.48786	.48786	.96
.45	.5	.9881	0.385	.49695	.49695	.99
.5	.4962	1.0	0.091	.5	.5	1.0
.55	.4846	.9971	-0.211	.495	.49674	.99
.6	.4653	.9786	-0.532	.48	.48624	.96
.65	.4383	.9434	-0.885	.455	.46740	.91
.7	.4035	.8892	-1.295	.42	.43912	.84
.75	.3612	.8121	-1.813	.375	.40031	.75
.8	.3110	.7027	-2.712	.32	.34988	.64
.85	.2532	.5425	-3.523	.255	.28673	.51
.9	.1877	.3586	-3.768	.18	.20976	.36
.95	.1143	.1713	-3.668	.095	.11788	.19
.975	.0748	.0823	-3.441	.04875	.06601	.0975
1.0	.0333	0	-3.003	0	.01	0

NACA 16 with parabolic (trim TE)　　NACA 16

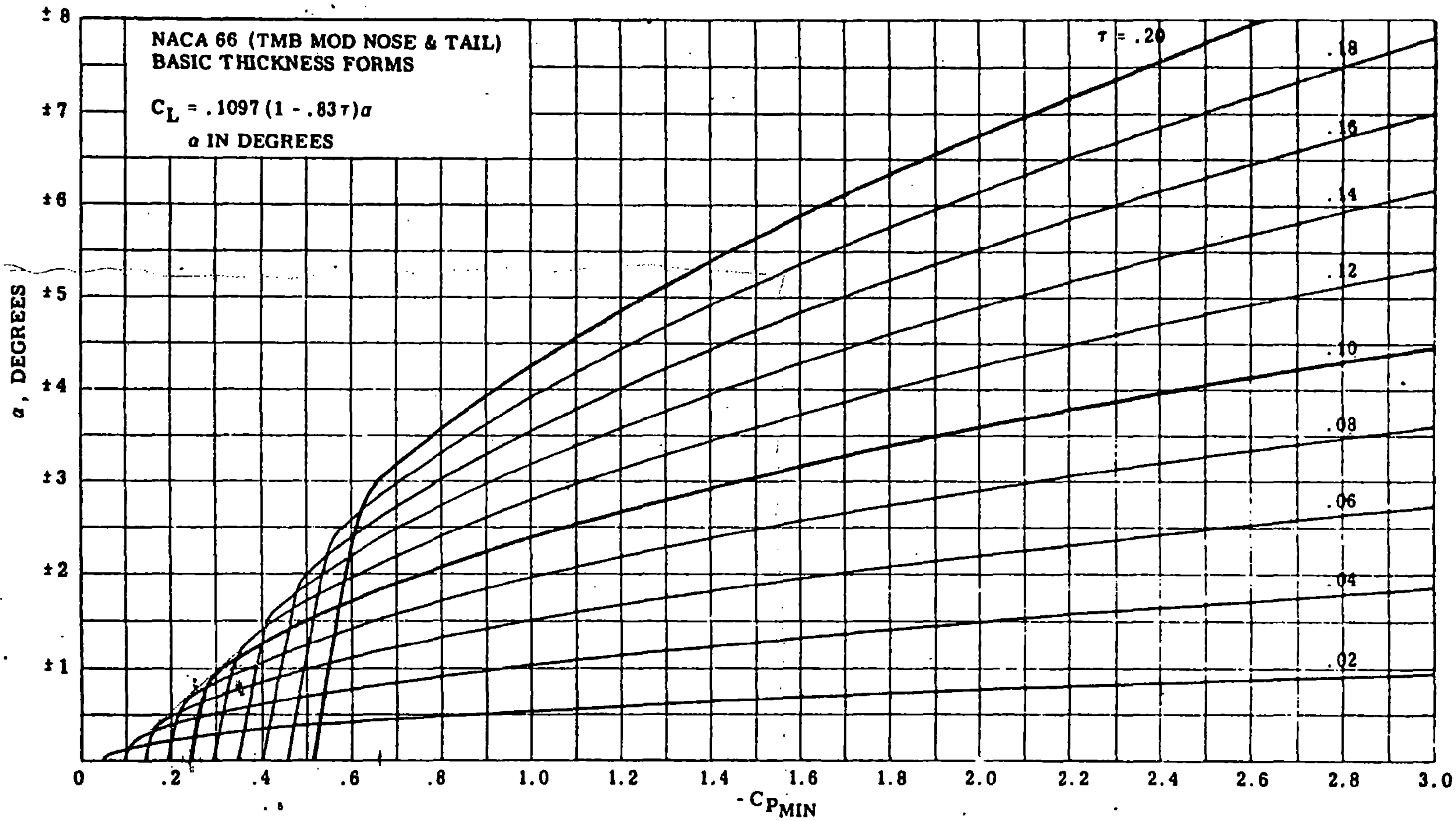

Figure 5 - Minimum Pressure Envelopes for NACA 66 Sections (TMB Modified Nose and Tail) with Zero Camber

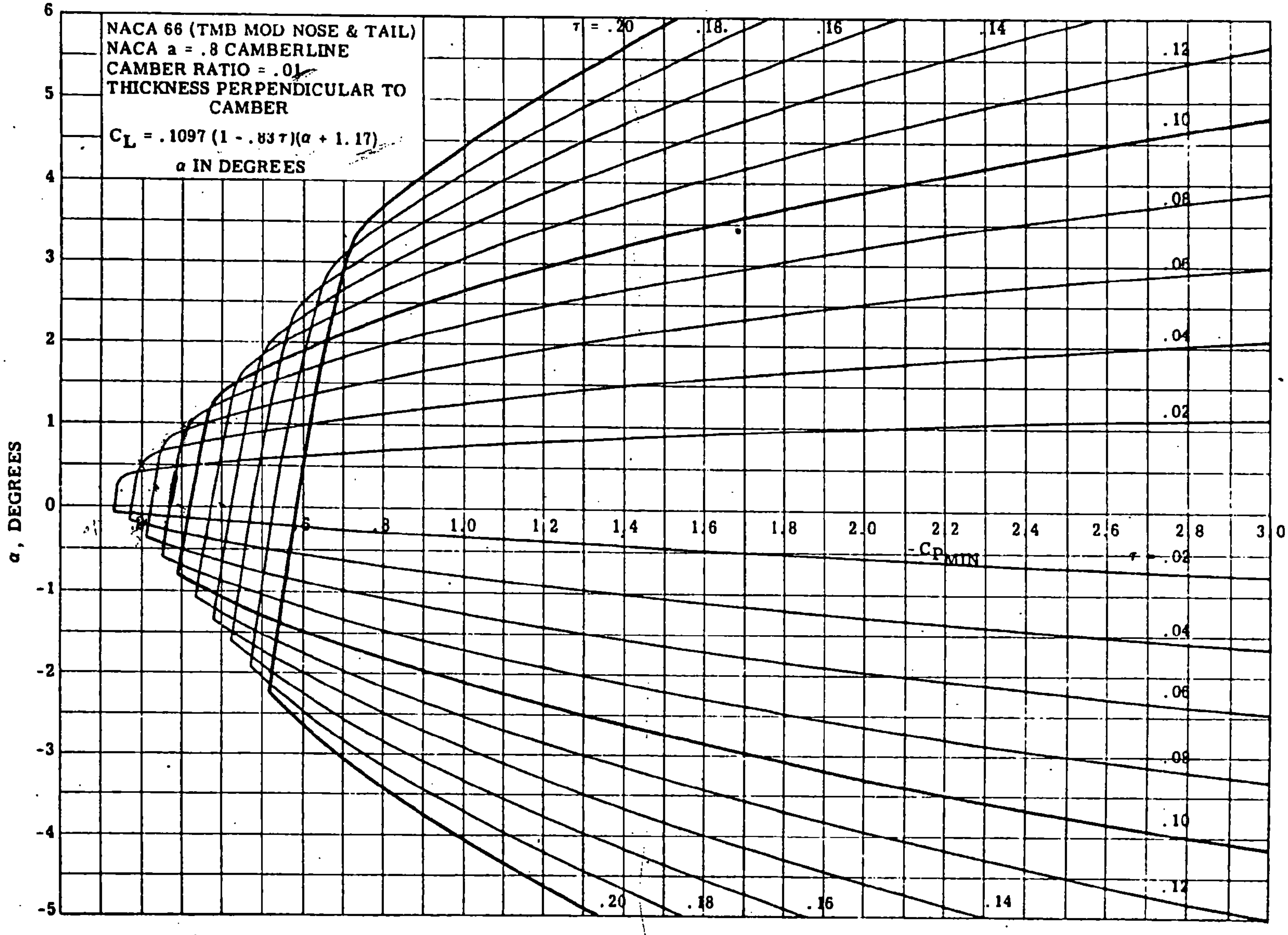

Figure 6 - Minimum Pressure Envelopes for NACA 66 Sections (TMB Modified Nose and Tail) with the NACA a = 0.8 Camberline, Having a Maximum Camber Ratio of 0.01

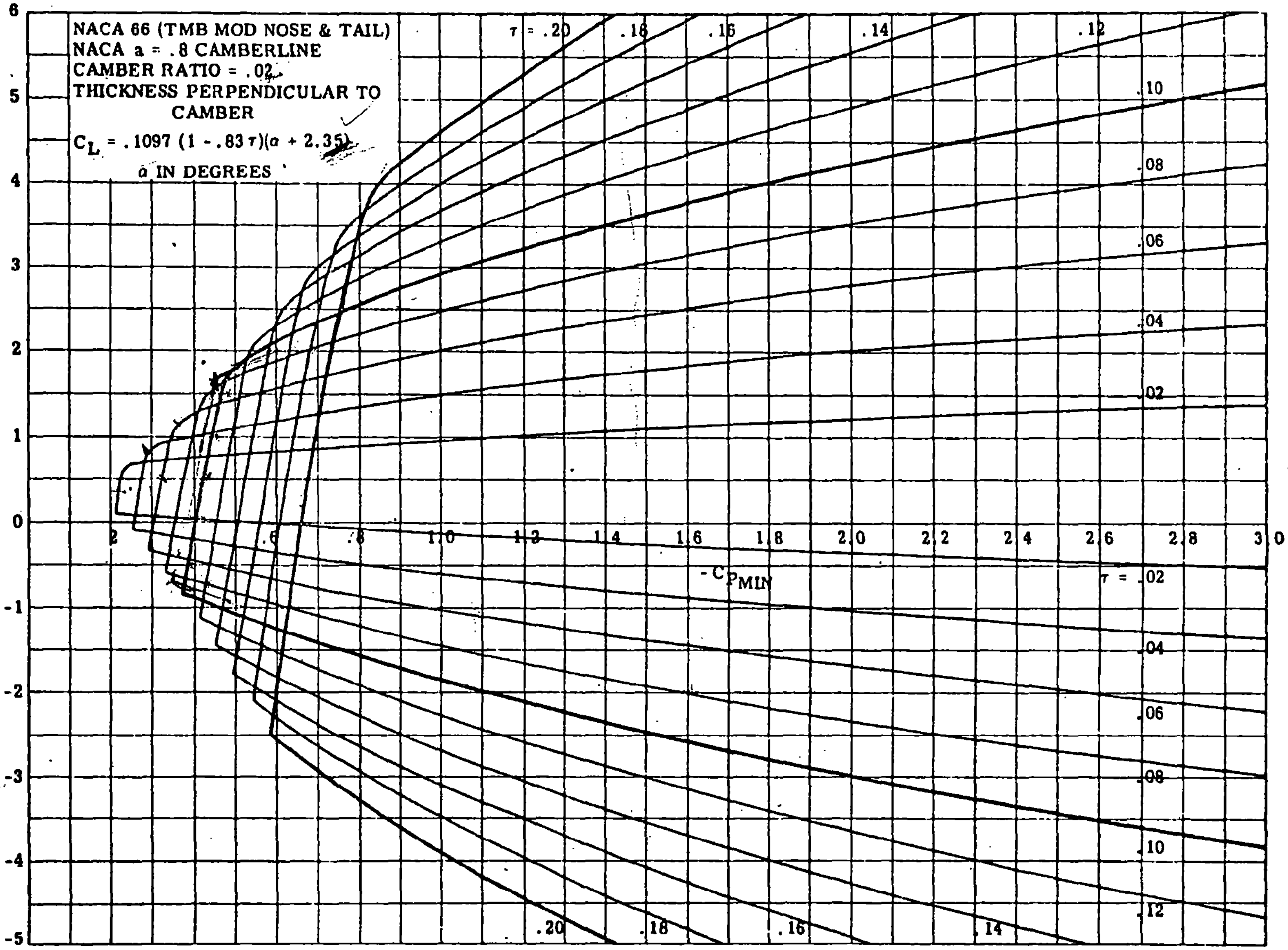

Figure 7 - Minimum Pressure Envelopes for NACA 66 Sections (TMB Modified Nose and Tail) with the NACA a = 0.8 Camberline, Having a Maximum Camber Ratio of 0.02

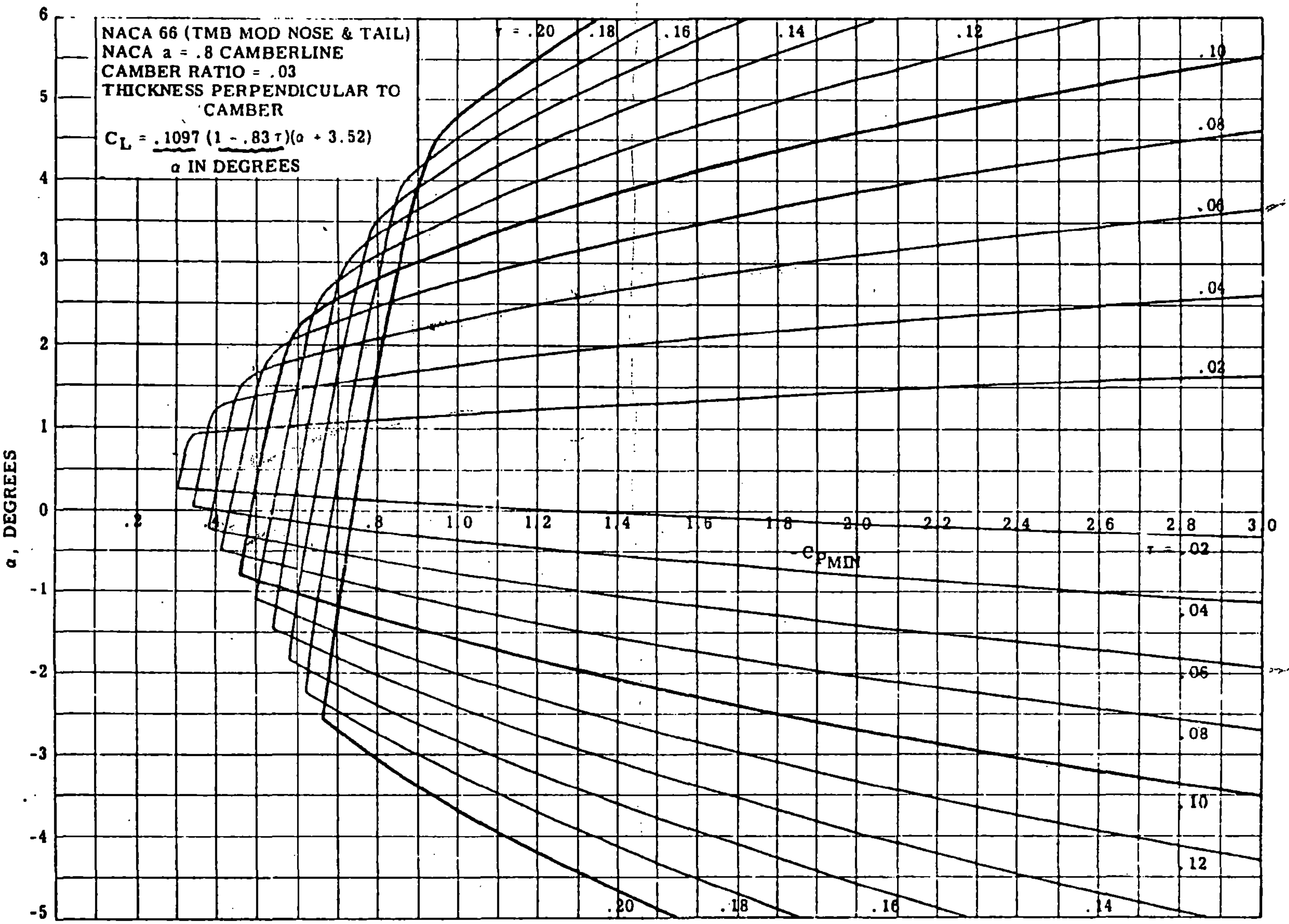

Figure 8 - Minimum Pressure Envelopes for NACA 66 Sections (TMB Modified Nose and Tail) with the NACA a = 0.8 Camberline, Having a Maximum Camber Ratio of 0.03

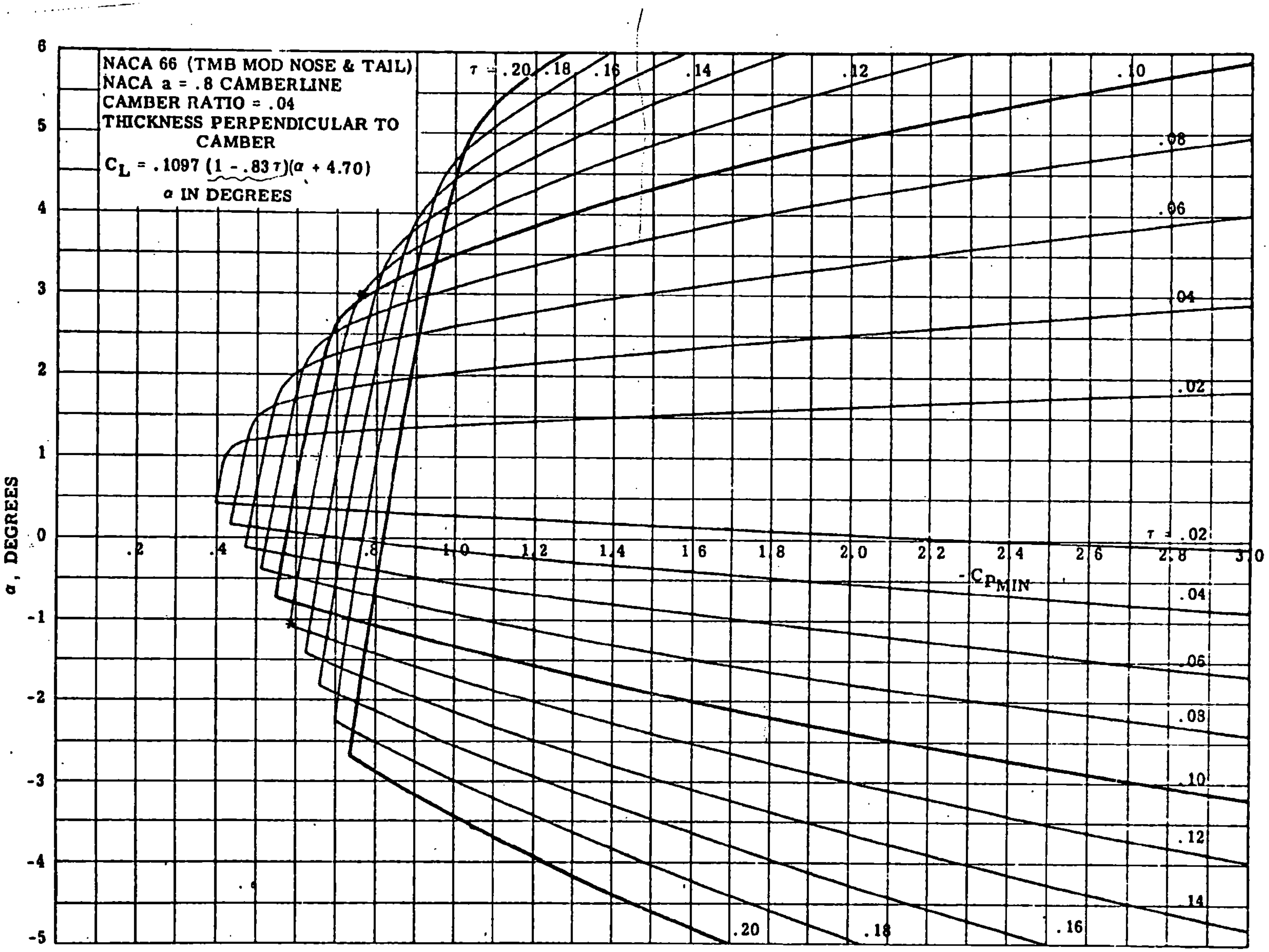

Figure 9 - Minimum Pressure Envelopes for NACA 66 Sections (TMB Modified Nose and Tail) with the NACA a = 0.8 Camberline, Having a Maximum Camber Ratio of 0.04

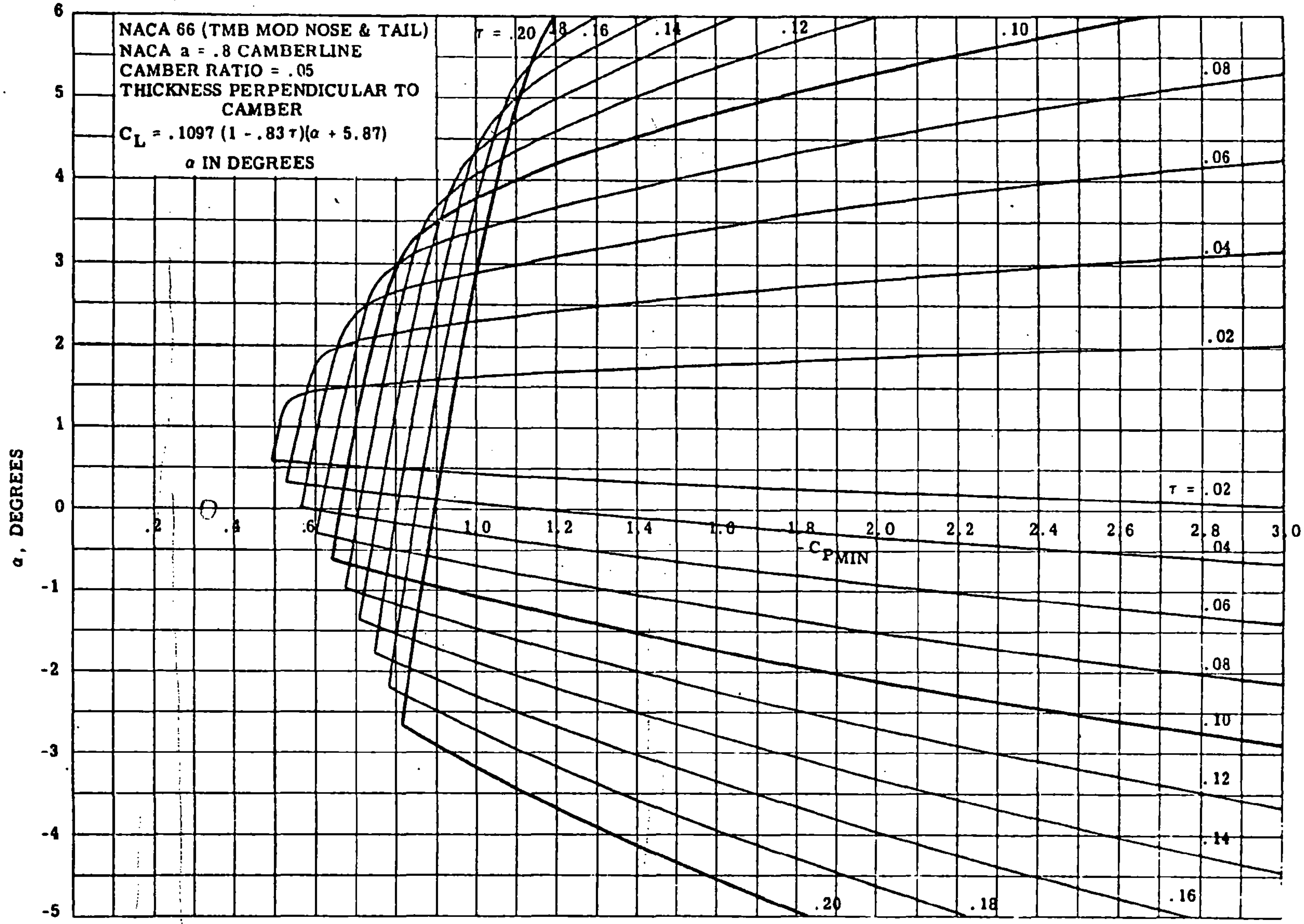

Figure 10 - Minimum Pressure Envelopes for NACA 66 Sections (TMB Modified Nose and Tail) with the NACA a = 0.8 Camberline, Having a Maximum Camber Ratio of 0.05

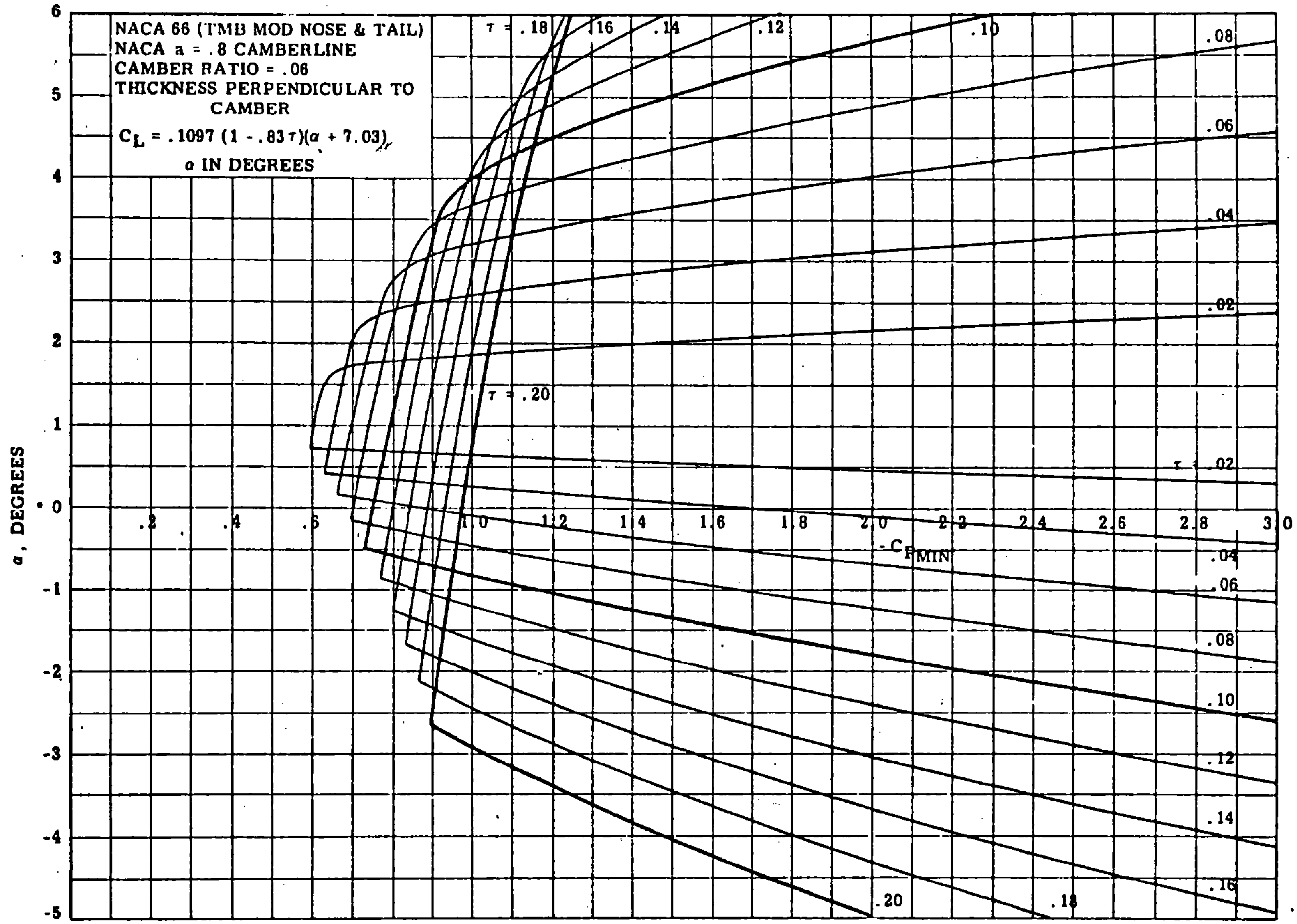

Figure 11 - Minimum Pressure Envelopes for NACA 66 Sections (TMB Modified Nose and Tail) with the NACA a = 0.8 Camberline, Having a Maximum Camber Ratio of 0.06

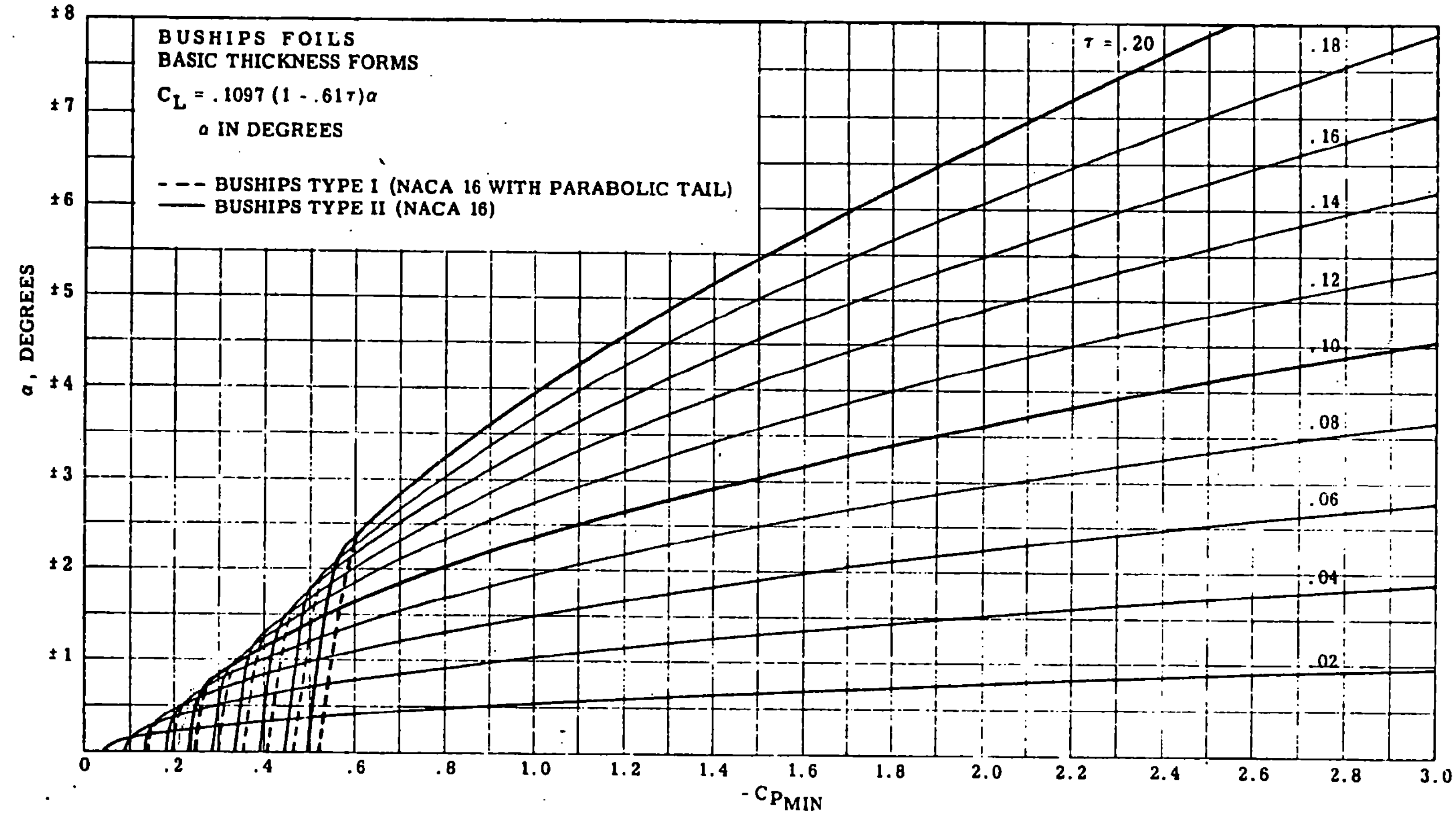

Figure 12 - Minimum Pressure Envelopes for the BuShips Type I and Type II Sections with Zero Camber

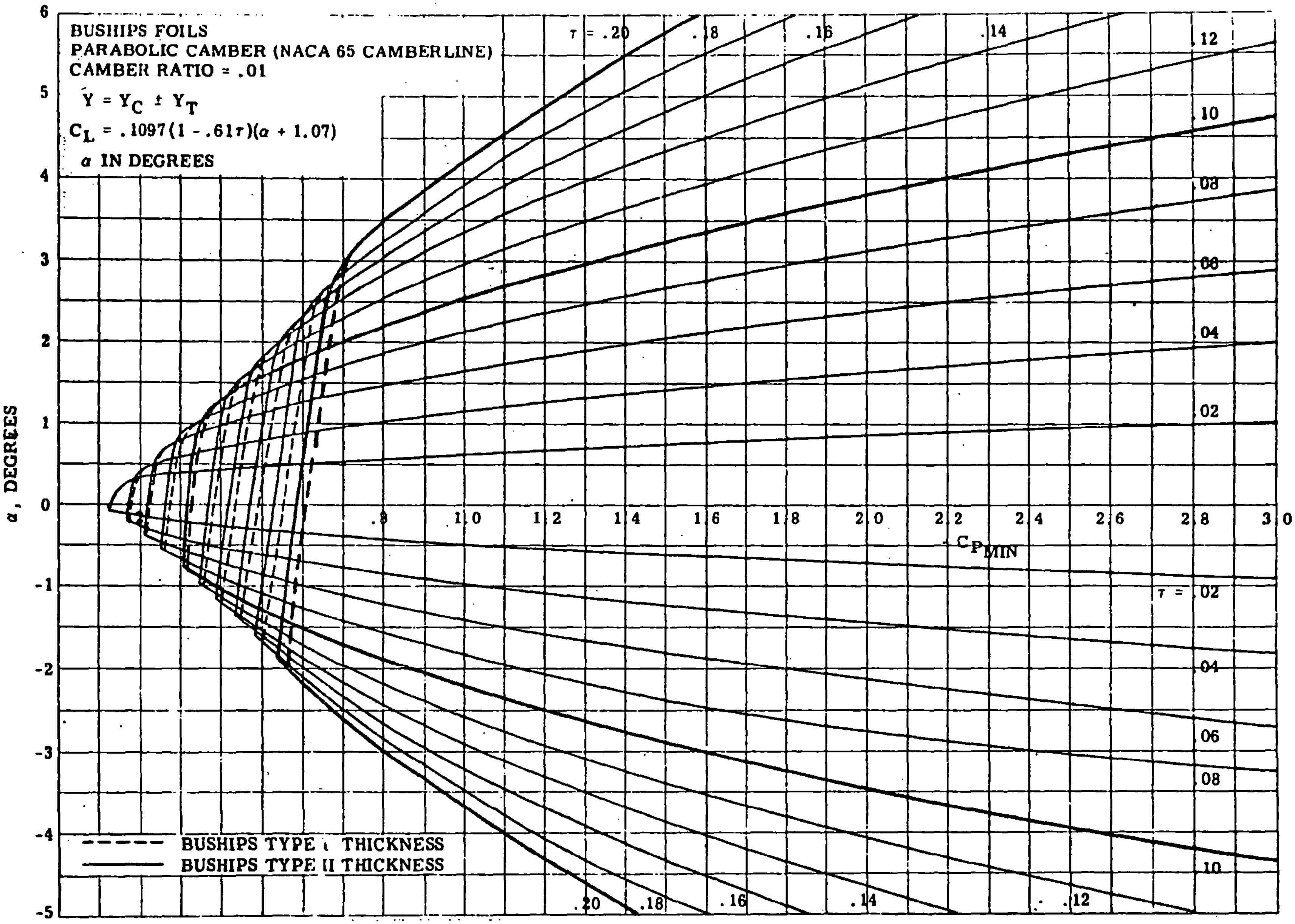

Figure 13 - Minimum Pressure Envelopes for the BuShips Type I and Type II Sections Having a Maximum Camber Ratio of 0.01

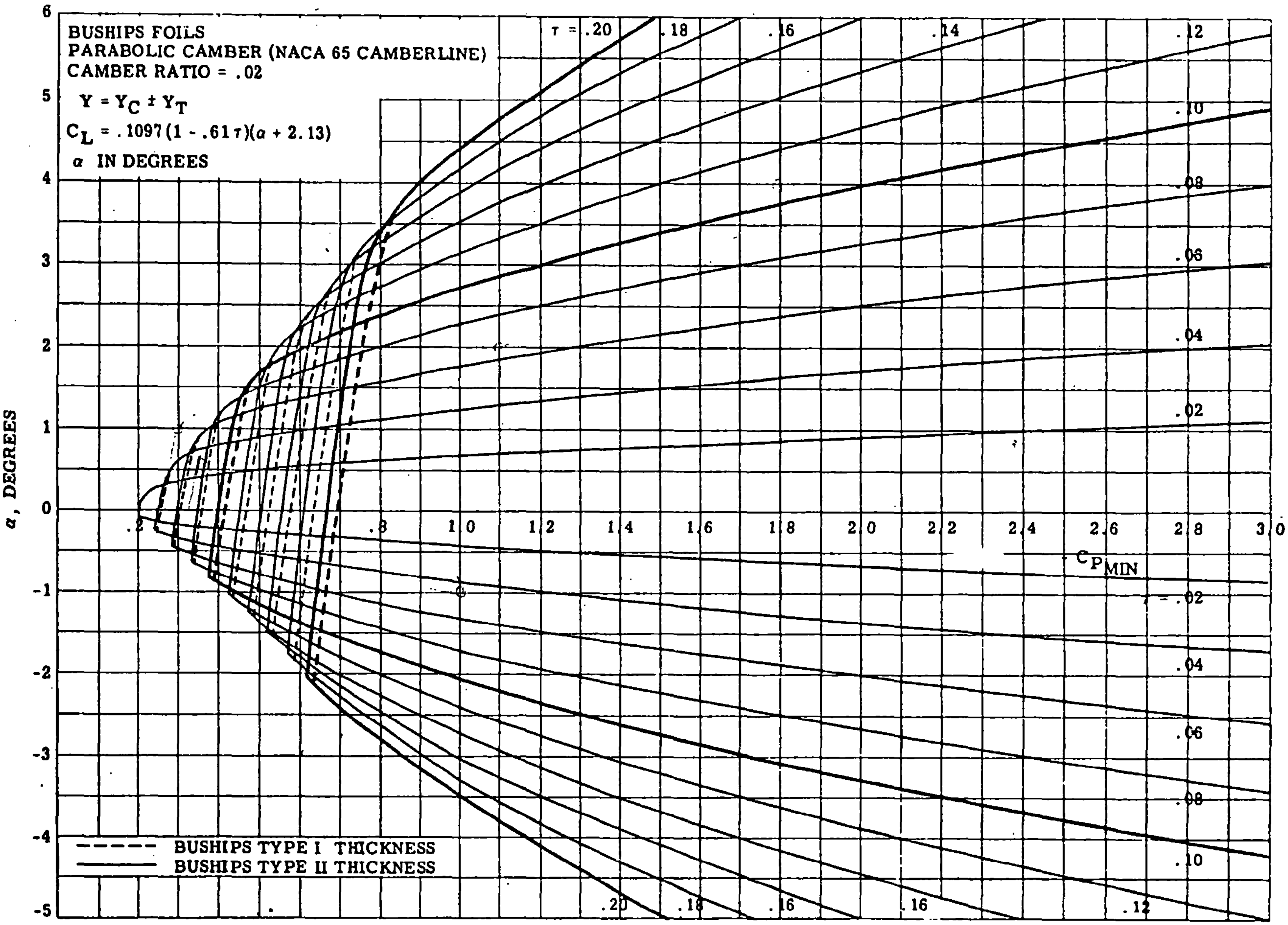

Figure 14 - Minimum Pressure Envelopes for the BuShips Type I and Type II Sections Having a Maximum Camber Ratio of 0.02

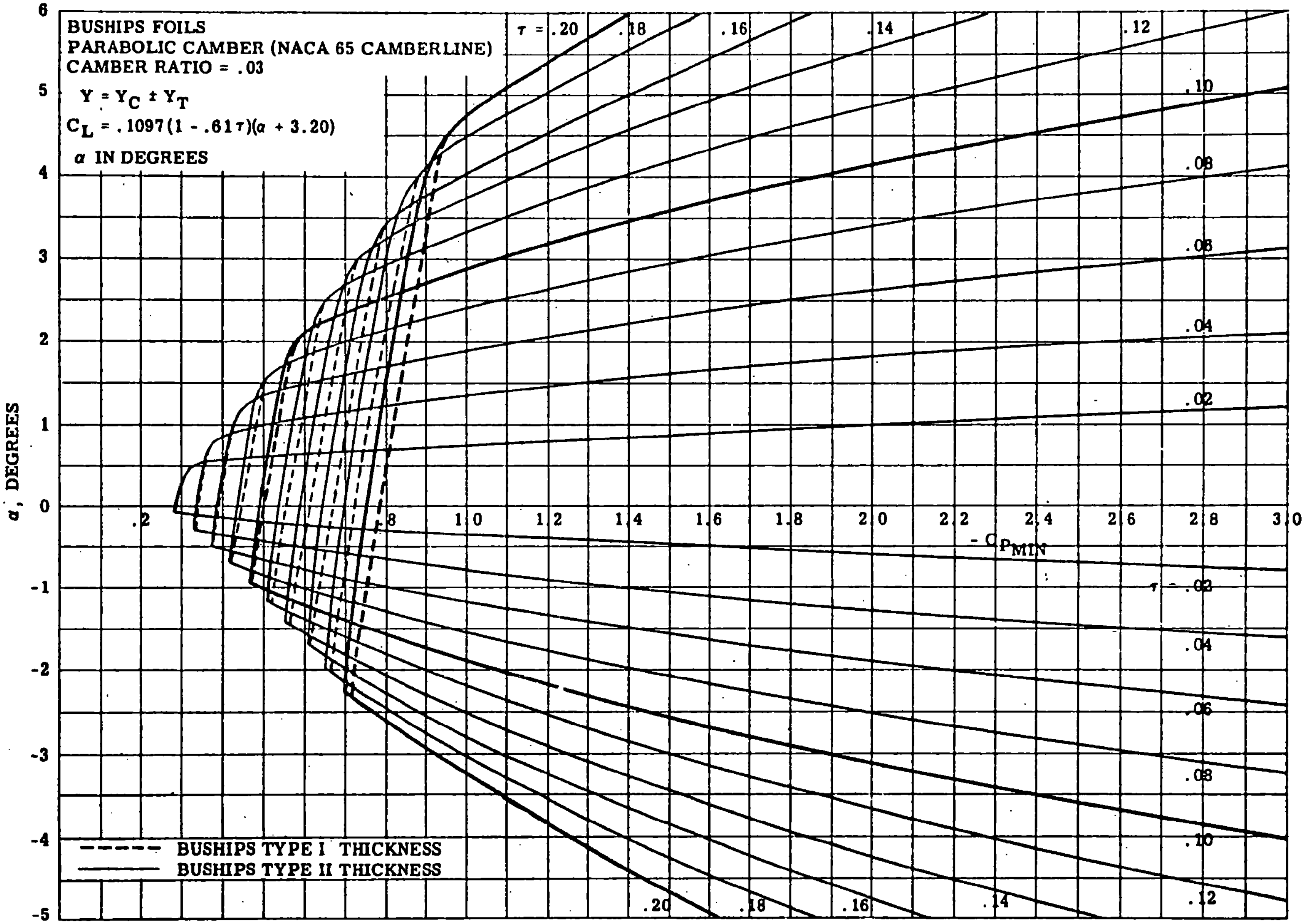

Figure 15 - Minimum Pressure Envelopes for the BuShips Type I and Type II Sections Having a Maximum Camber Ratio of 0.03

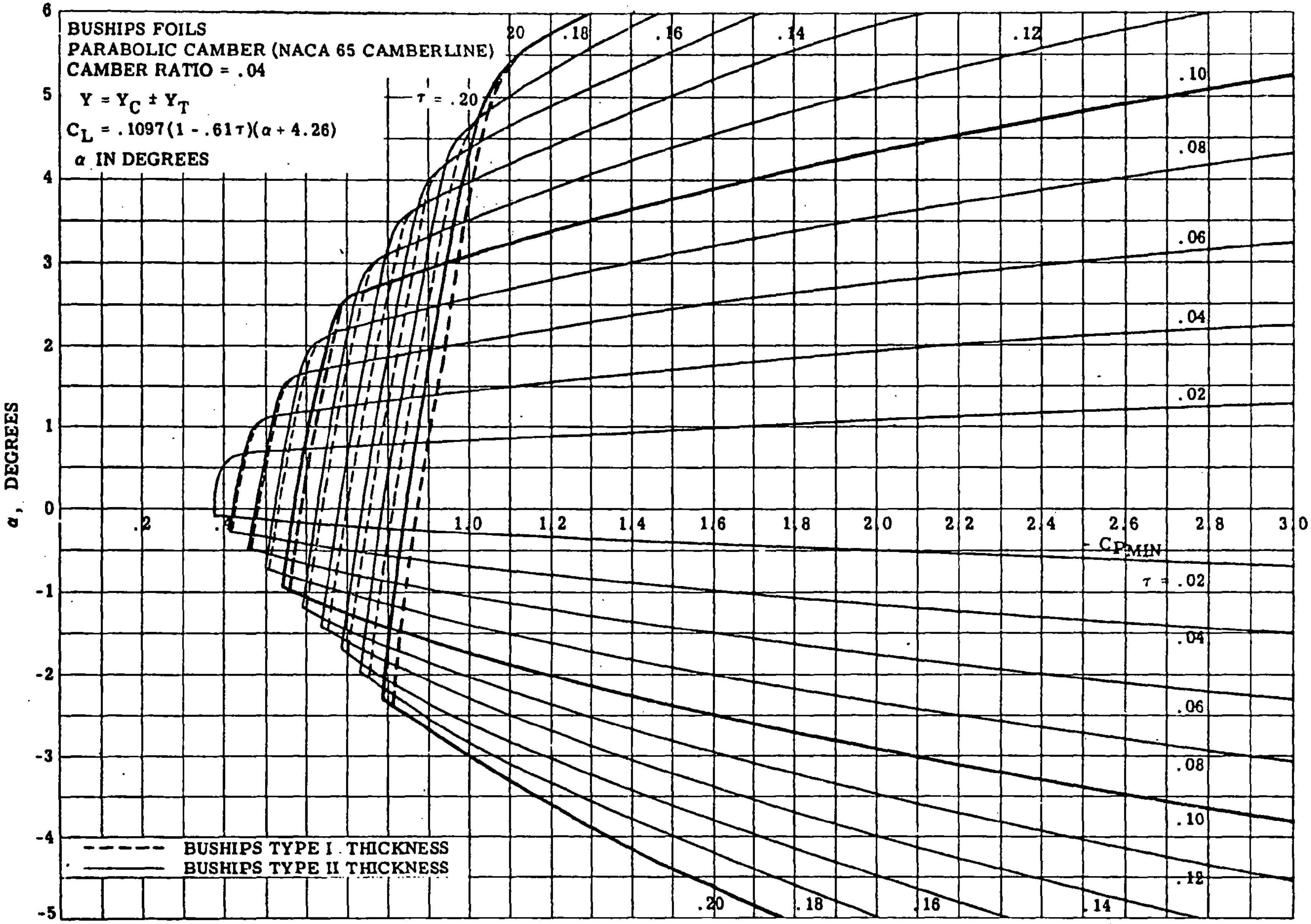

Figure 16 - Minimum Pressure Envelopes for the BuShips Type I and Type II Sections Having a Maximum Camber Ratio of 0.04

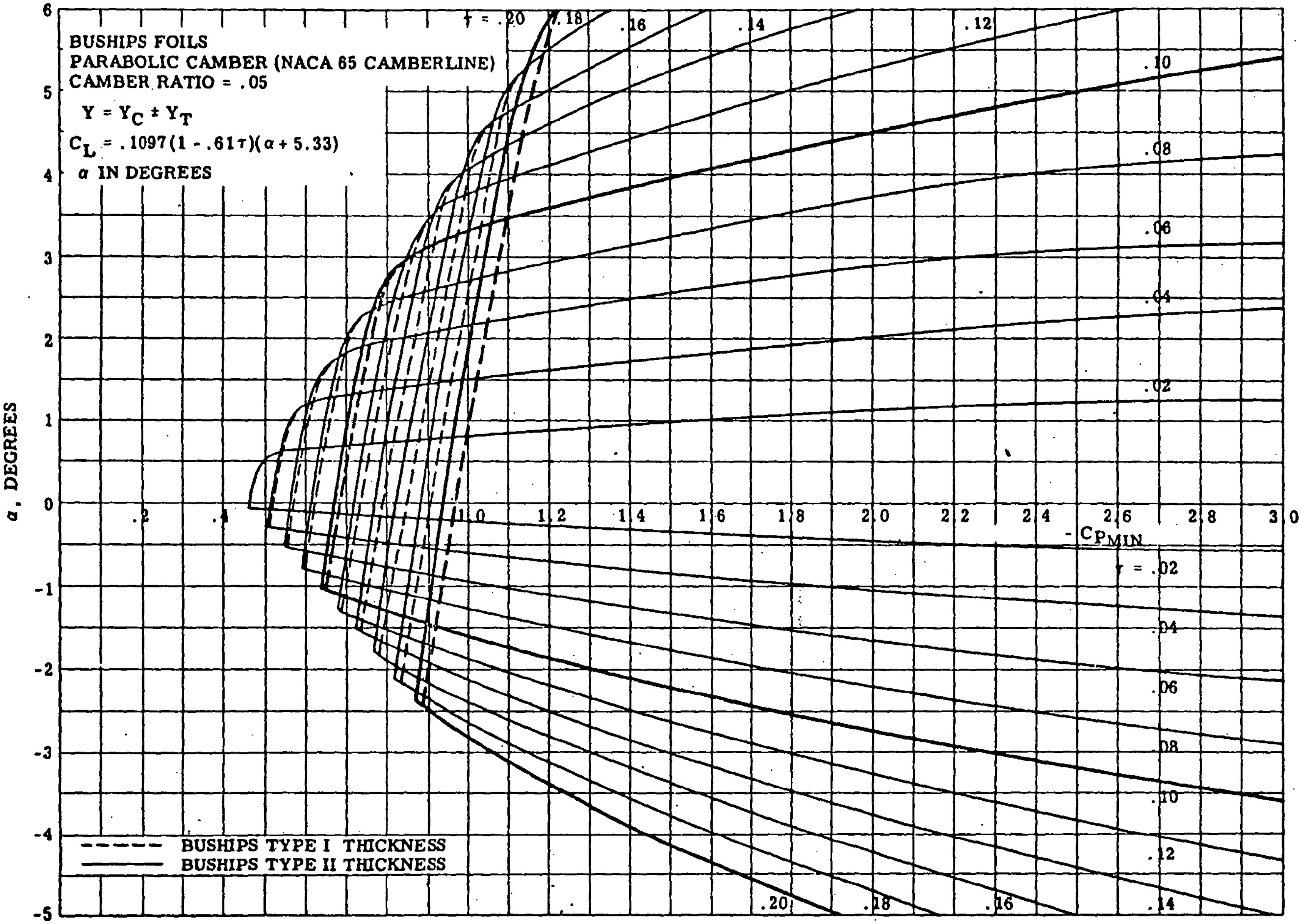

Figure 17 - Minimum Pressure Envelopes for the BuShips Type I and Type II Sections Having a Maximum Camber Ratio of 0.05

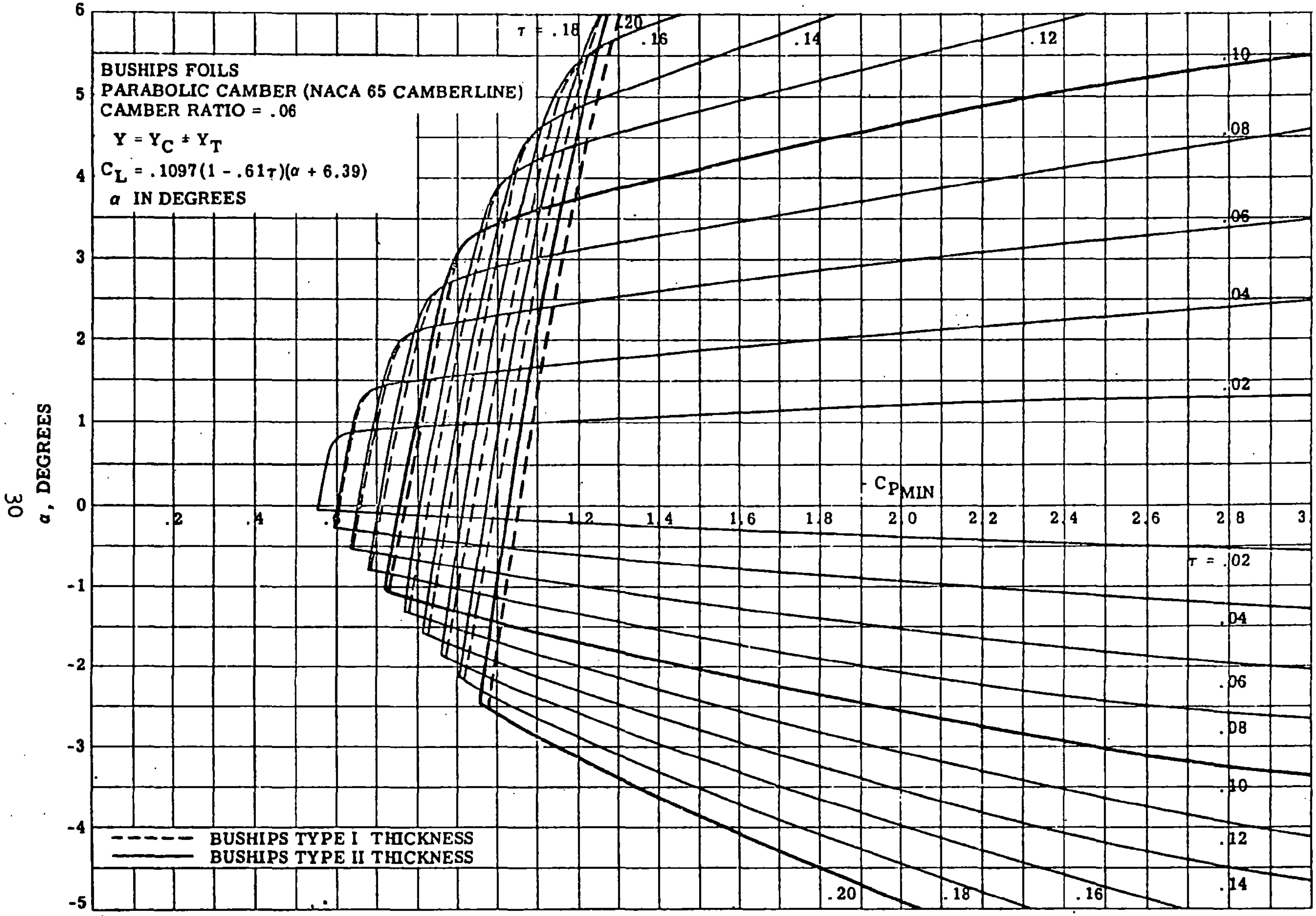

Figure 18 - Minimum Pressure Envelopes for the BuShips Type I and Type II Sections Having a Maximum Camber Ratio of 0.06

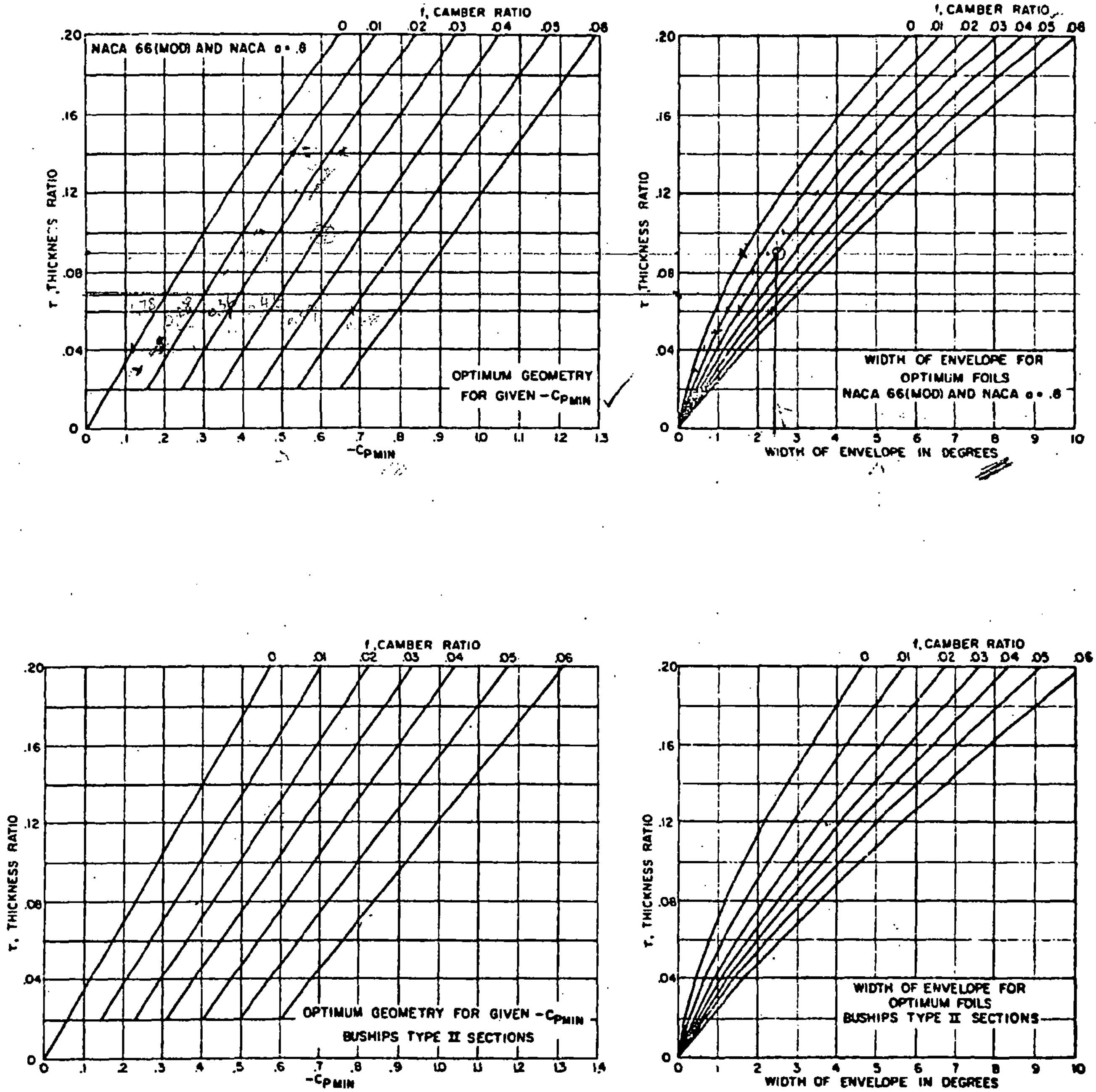

Figure 19 - Geometry of Optimum Foils

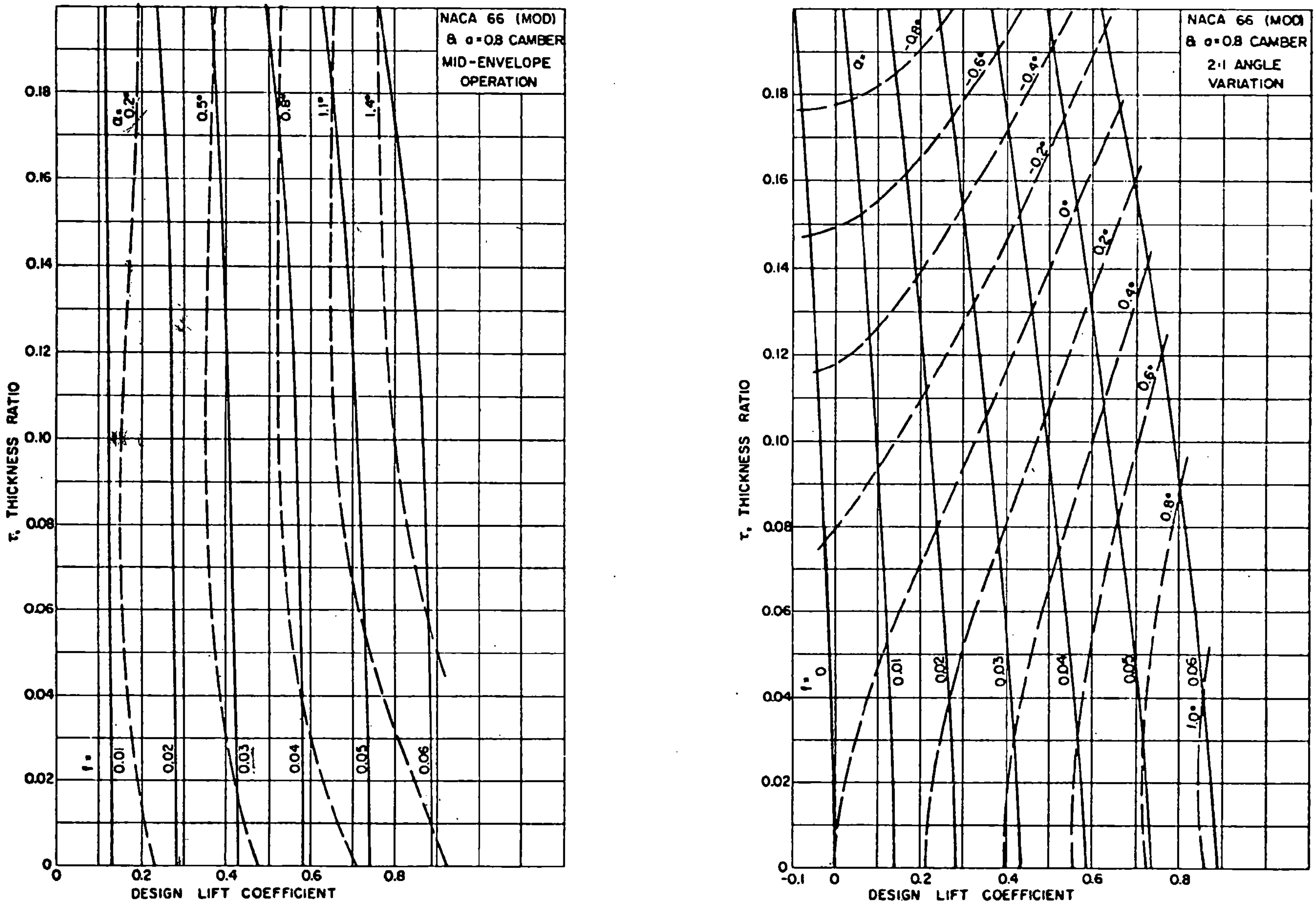

Figure 20 - Design Incidence and Lift Coefficient for Optimum Foils, NACA 66 (TMB Modified Nose and Tail) Sections with NACA a = 0.8 Camber

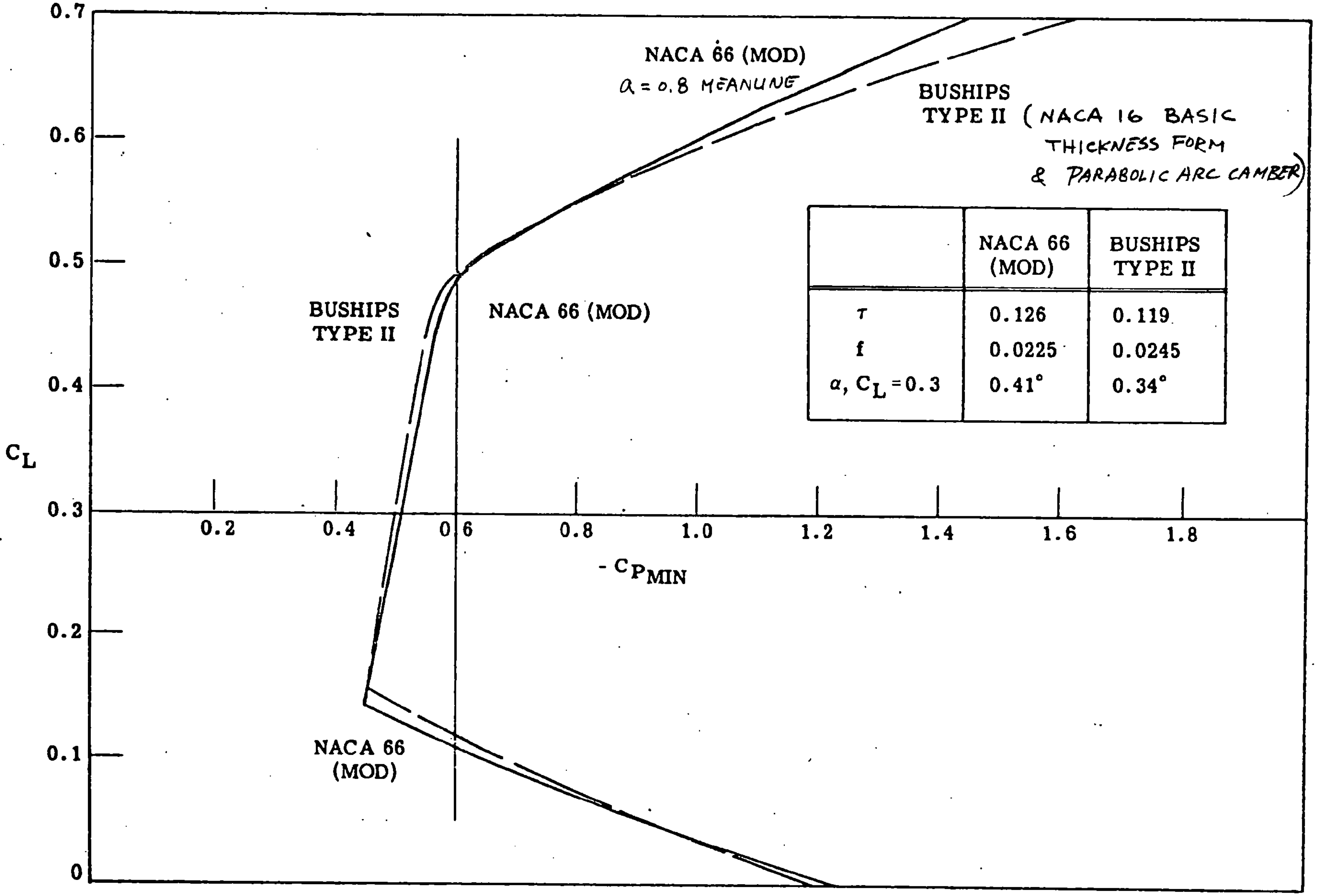

Figure 22 - Comparison of Foils Designed for an Average Lift Coefficient of 0.3 and Cavitation Number of 0.6

From " T. Brockett NSRDC Report 1780" Feb. 1966

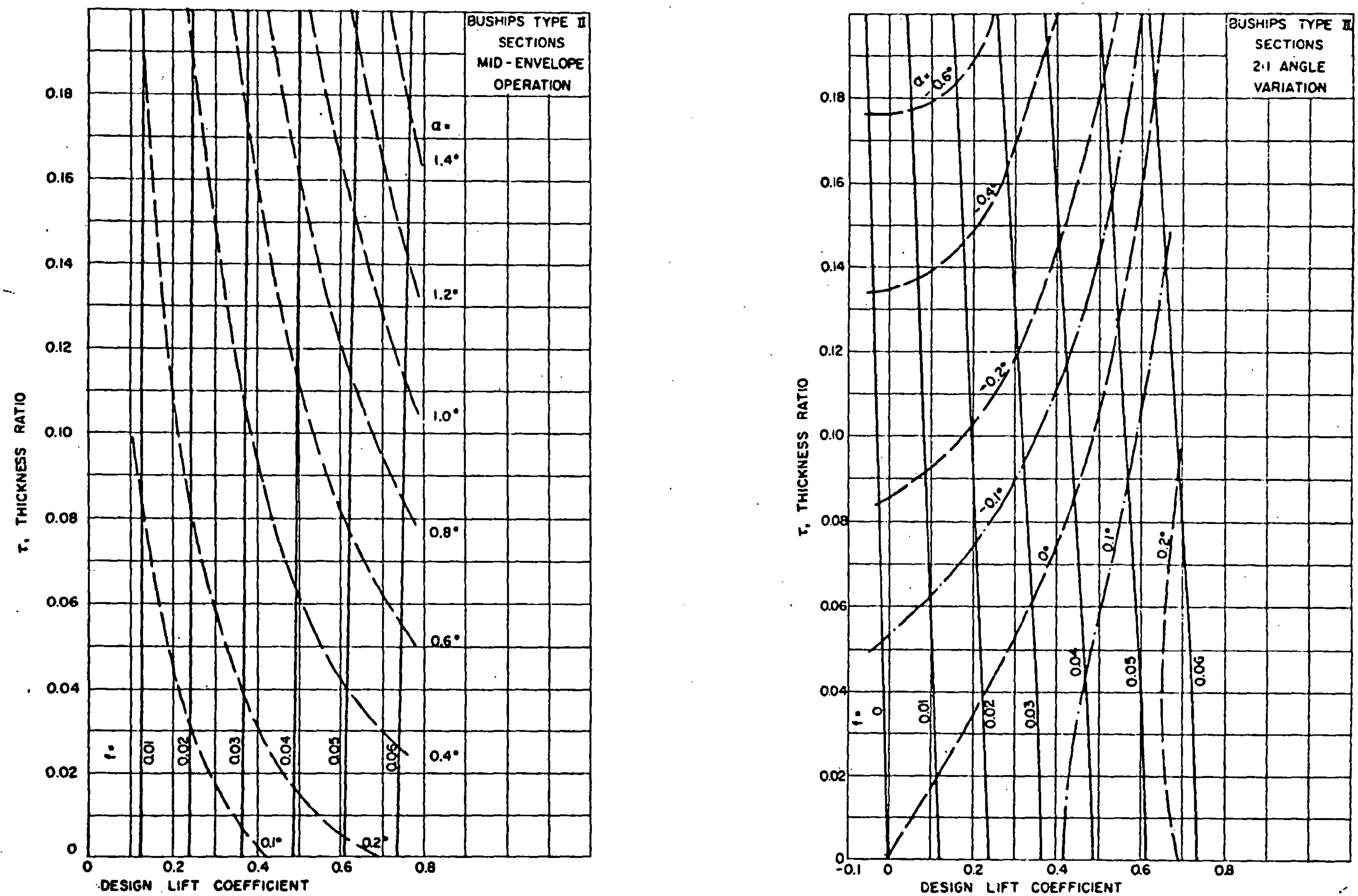

Figure 21 - Design Incidence and Lift Coefficients for Optimum Foils, BuShips Type II Sections